

New results on the N^* parameters from the
reaction of the two pion
photo- and electroproduction off the proton

E. Golovach

SINP MSU

EMIN 2015

Plan:

✓ *Physics Motivation:*

N studies in double pion photo- and electroproduction with CLAS*

✓ *Evaluation of the $\gamma p \rightarrow p \pi^+ \pi^-$ exclusive cross section from the CLAS data*

✓ *Resonance photocouplings extraction*

✓ *Evidence for the new baryon state $N'(1720)3/2+$*

✓ *Conclusion and outlook*

N studies in $\pi^+\pi^-$ photo- and electro prod with CLAS*

The main goals:

- ✓ *Explore the spectrum and structure of N^* at $W > 1.6$ GeV
Extracting the photo/electrocouplings of N^* and improving the knowledge on their $\pi\Delta$ and ρp decay widths*
- ✓ *Search for the new baryon states*
- ✓ *Important contributions in the exploration of the strong interaction in the non perturbative regime of QCD through the spectrum and electrocoupling of excited nucleon states*

V.D.Burkert, Int.J.Mod.Phys. 26, 1460050 (2014)

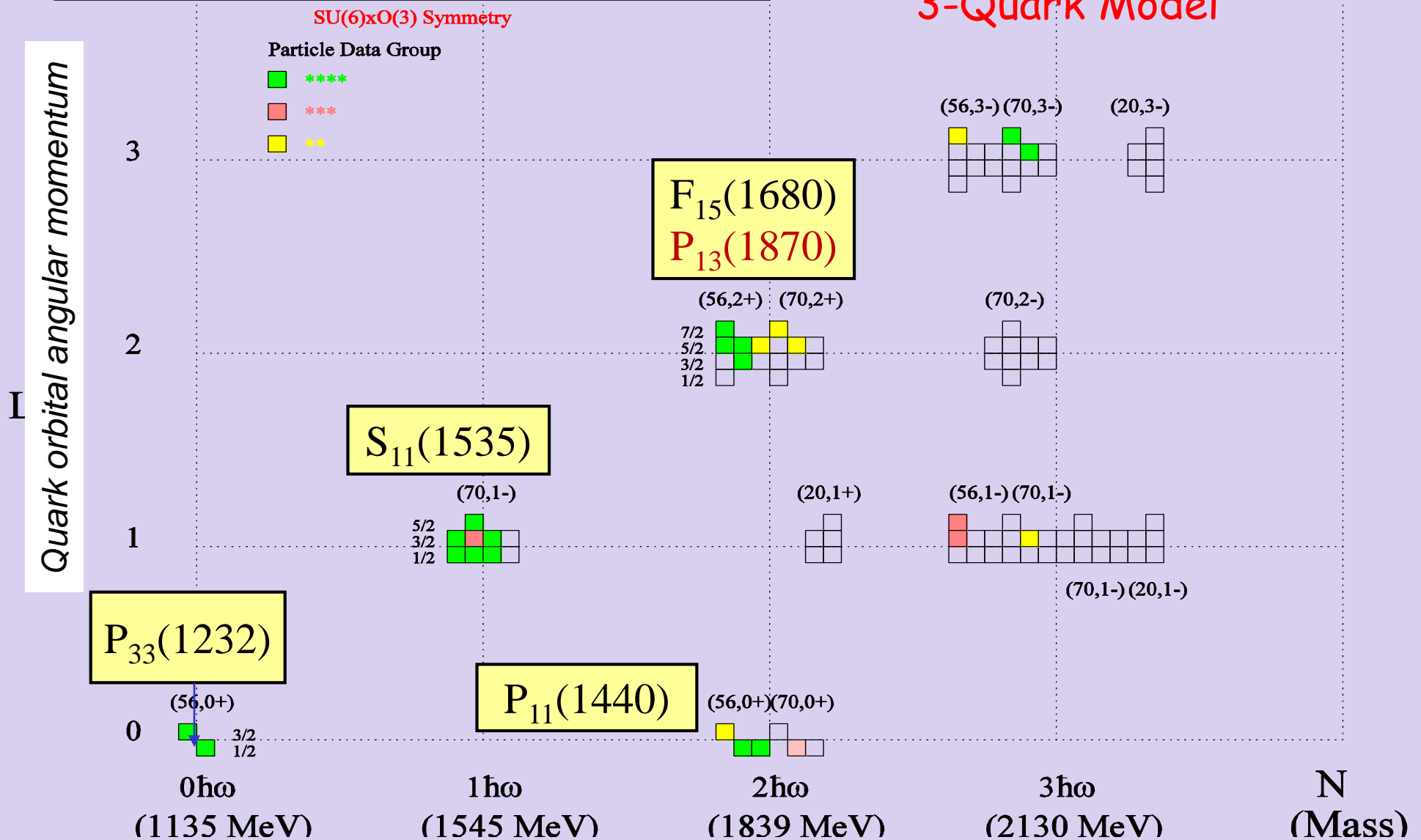
I.C. Cloët and C.D. Roberts, Prog. Part. Nucl. Phys. 77, 1 (2014).

Moiseev V.I. et al. arXiv 1508.04088 [nucl.ex]

"Missing" baryon states

SU(6): Spin-flavor symmetry of QCD

3-Quark Model



HO-Model Principal Energy Levels in the SU(6)xO(3) classification of baryons

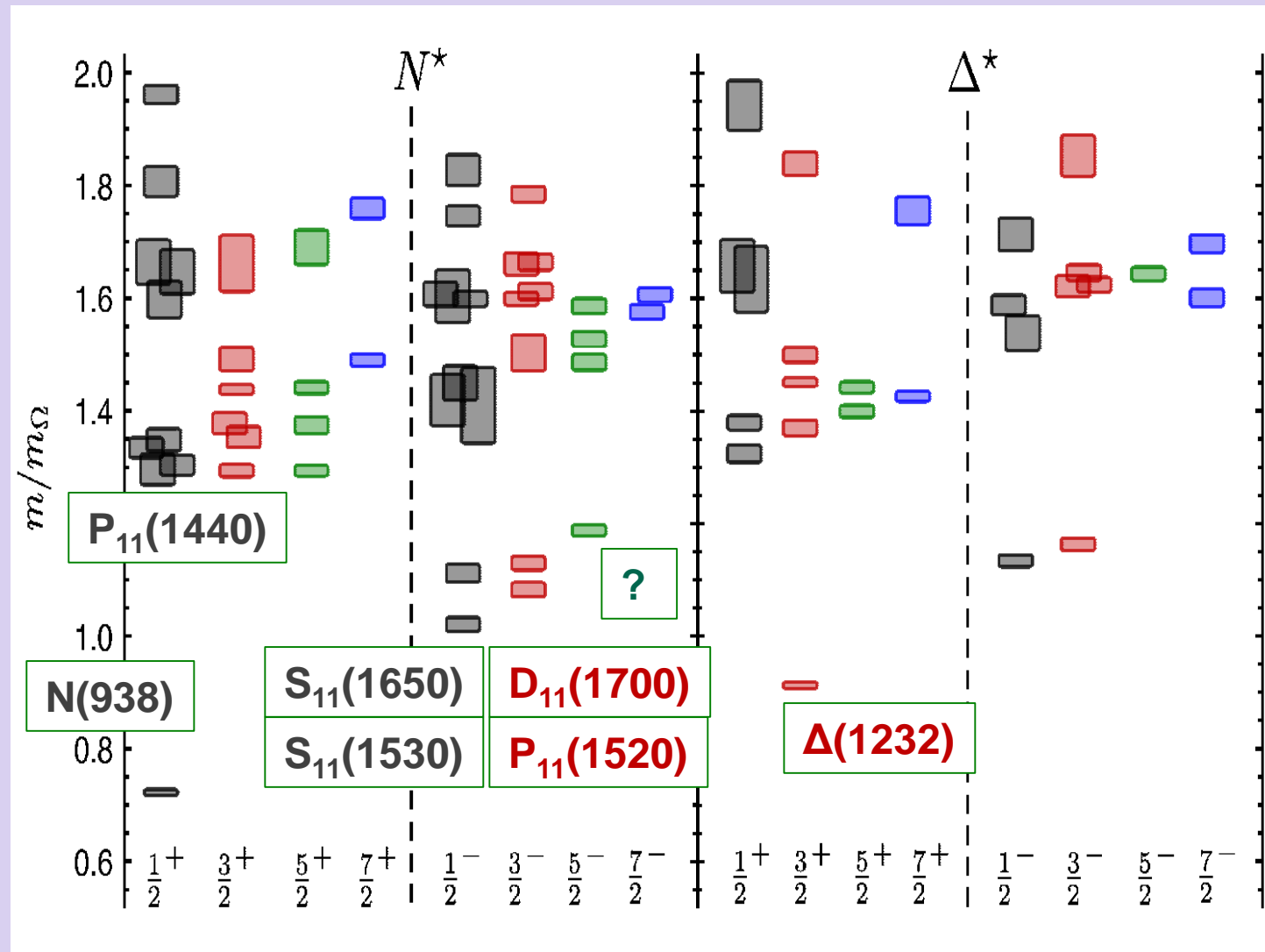
N^* spectrum in Lattice QCD calculation

$m_\pi = 396$ MeV

LQCD N^* spectrum:

Support for SU(6) spin-flavor symmetry employed in constituent quark models (CQM). Lattice calculations suggest existence of as many “missing” N^* states as expected in CQM

Hybrid baryons in mass range >1.9 GeV



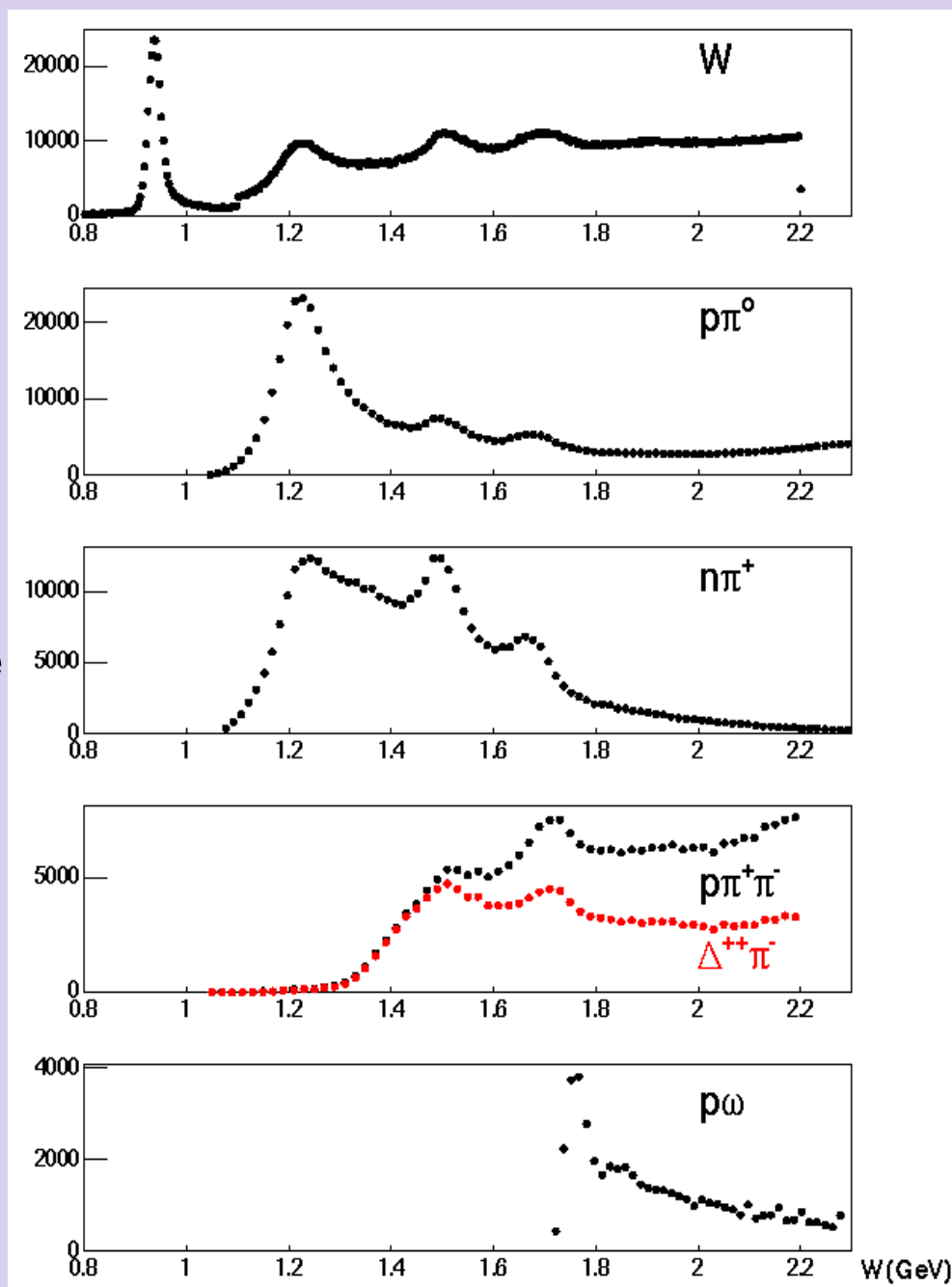
*R. Edwards, et al.,
PRD 84(2011)074508*

The program of the N^* studies with CLAS

Consistent results on N^* photo/electro couplings obtained from independent analysis of the major exclusive channels are critical for reliable access to these parameters

The CLAS detector provided dominant part of information on all relevant in resonance regions exclusive channels for the first time

The πN and $\pi\pi N$ are two major contributors to the N^* excitation region. And the major source of information on the resonance photocouplings.



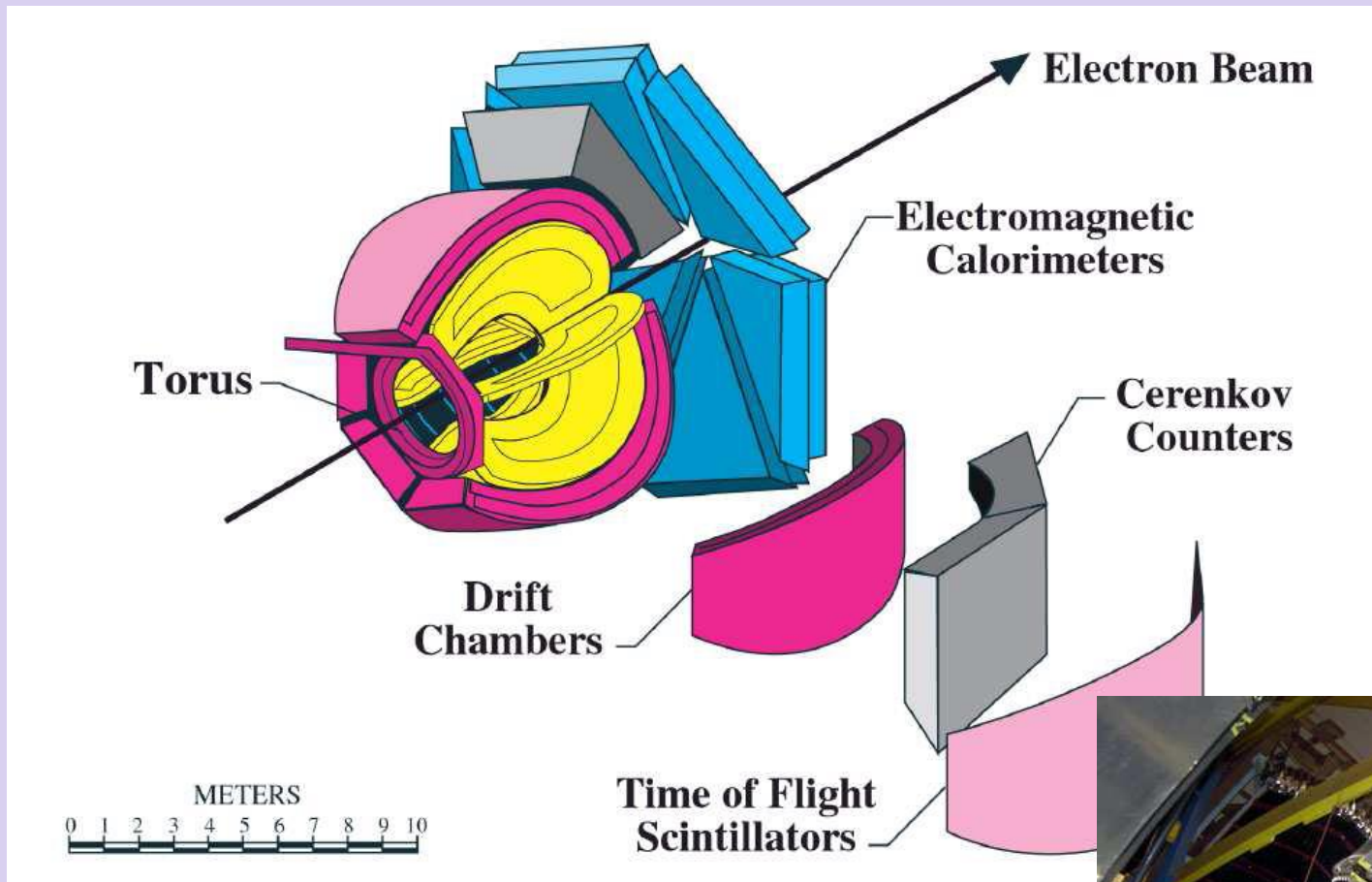
Why two pion photoproduction is important?

- Huge statistics of the CLAS g11 data. It allows to determine the relevant mechanism contributing to this channel.
- Sensitivity to the high-lying N^* , since most of N^* with masses more than 1.6 GeV decay preferably into two pions
- Promising opportunity for the “missing” baryon state search in combined analysis of two pion electro- and photoproduction

CLAS detector at JLAB

Superconducting
spectrometer

- ✓ $\sim 4\pi$ coverage
- ✓ Continuous $e\gamma$ beam up to ~ 5 GeV
- ✓ Detection of multiparticle final states



G11A Data set in JLAB

- ✓ *Continuous 60 nA electron beam $E=4$ GeV for 50 days*
- ✓ *Tagged photons: 1.6-3.8 GeV with 0.1% energy resolution*
- ✓ *LH2 target*
- ✓ *$\sim 2 \times 10^9$ two track triggers were collected*

Analysis of the reaction $\gamma p \rightarrow \pi^+ \pi^- p$

- ✓ *Charged particle identification. Kinematic Fit.*
- ✓ *Reliable acceptance area*
- ✓ *Detection Efficiency (Monte-Carlo simulations)*

Cross section extraction

The cross section for the reaction $\gamma p \rightarrow p \pi^+ \pi^-$.

The kinematics of the 3 particle finale state is described with 5 independent variables. Our choice is:

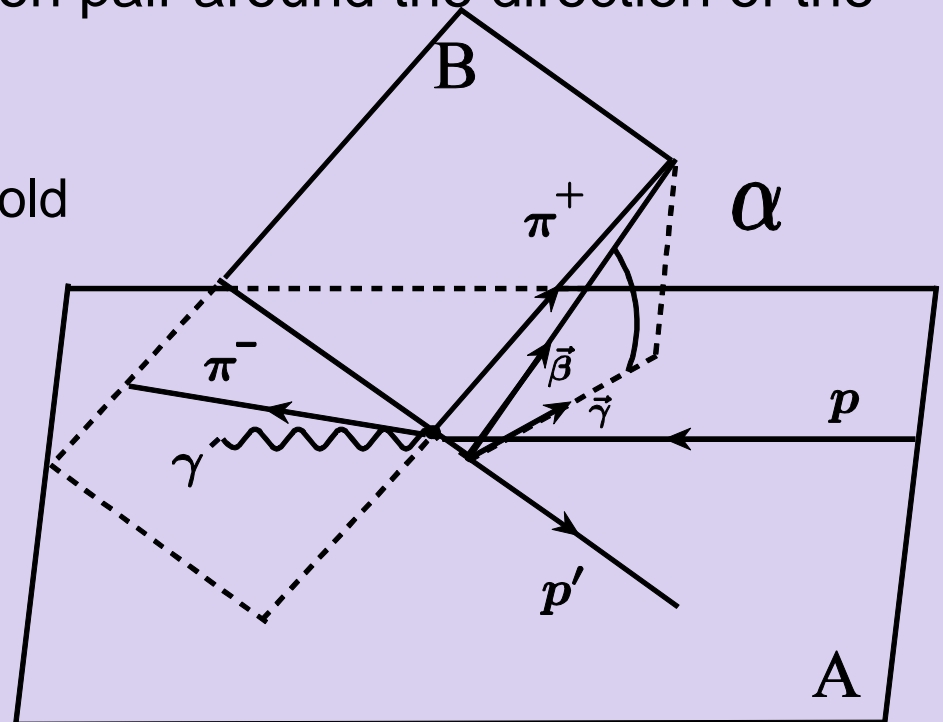
- two of three invariant masses, i.e. $M(p \pi^+)$ and $M(\pi^+ \pi^-)$
- two spherical angles θ and ϕ describing the direction of one of the final hadron
- α is rotation angle of the final hadron pair around the direction of the first hadron momentum

Due to the **high statistics of G11** the 1-fold and **2-fold** differential x-sections can be extracted in the W-bins of 25 MeV width

$$\frac{d\sigma}{dM_i}, \frac{d\sigma}{d\theta_j}, \frac{d\sigma}{d\alpha_j}, \frac{d^2\sigma}{dM_i d\theta_j} \dots$$

$$i = (p \pi^+), (\pi^+ \pi^-), (p \pi^-)$$

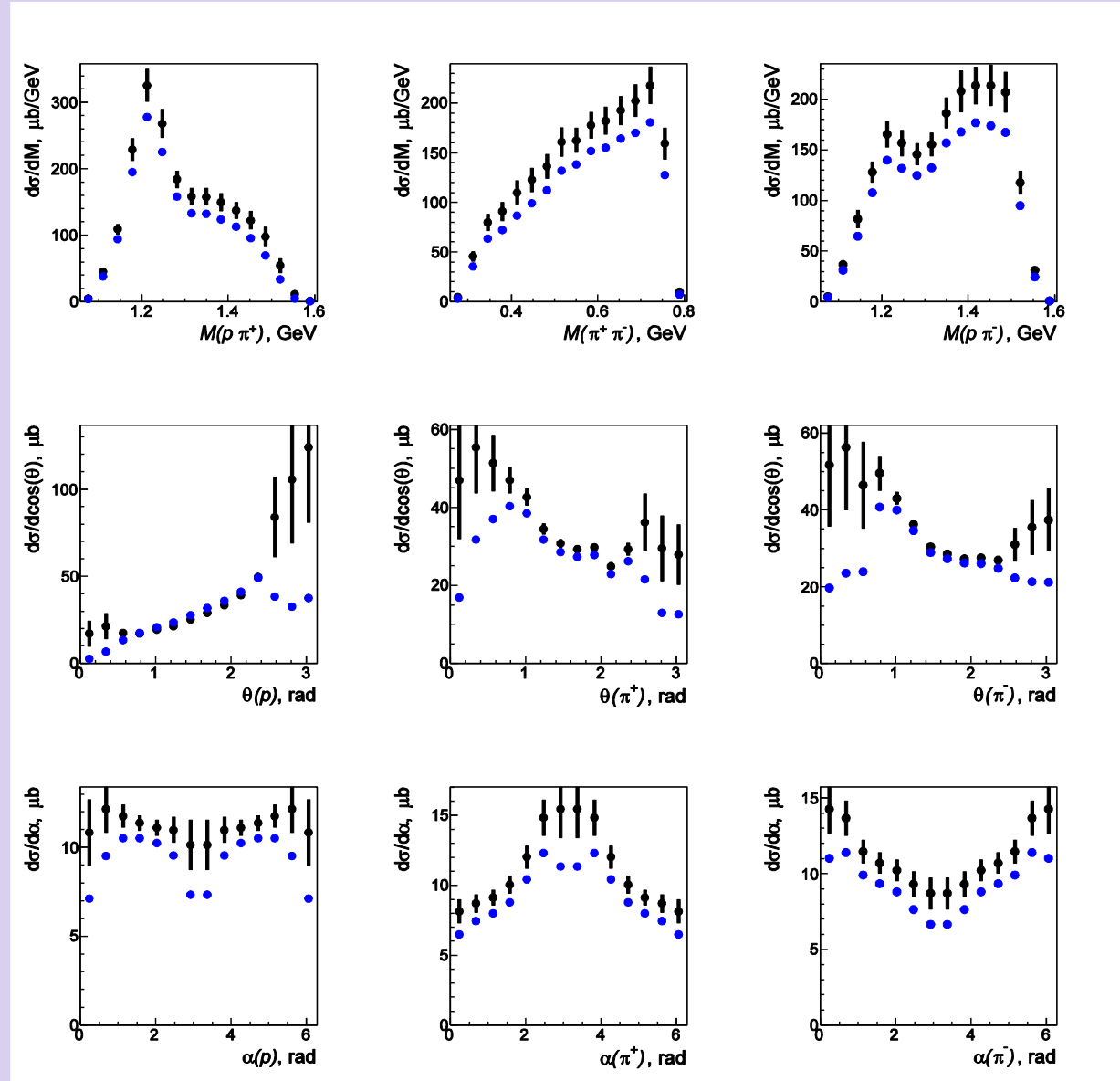
$$j = p, \pi^+, \pi^-$$



Dead zones: Simple approach

CLAS has dead zones. They are mainly located in forward and backward directions. Taking them into account is especially important in experiments with real photons.

Accounting for the dead zones is made in the following way: In each bin of one fold differential x-section the percentage of the dead zones from contributing multidimensional cells was evaluated as a ratio of the number of dead cells to the total number of contributing cells. Then the x-section can be corrected by dividing by this factor.



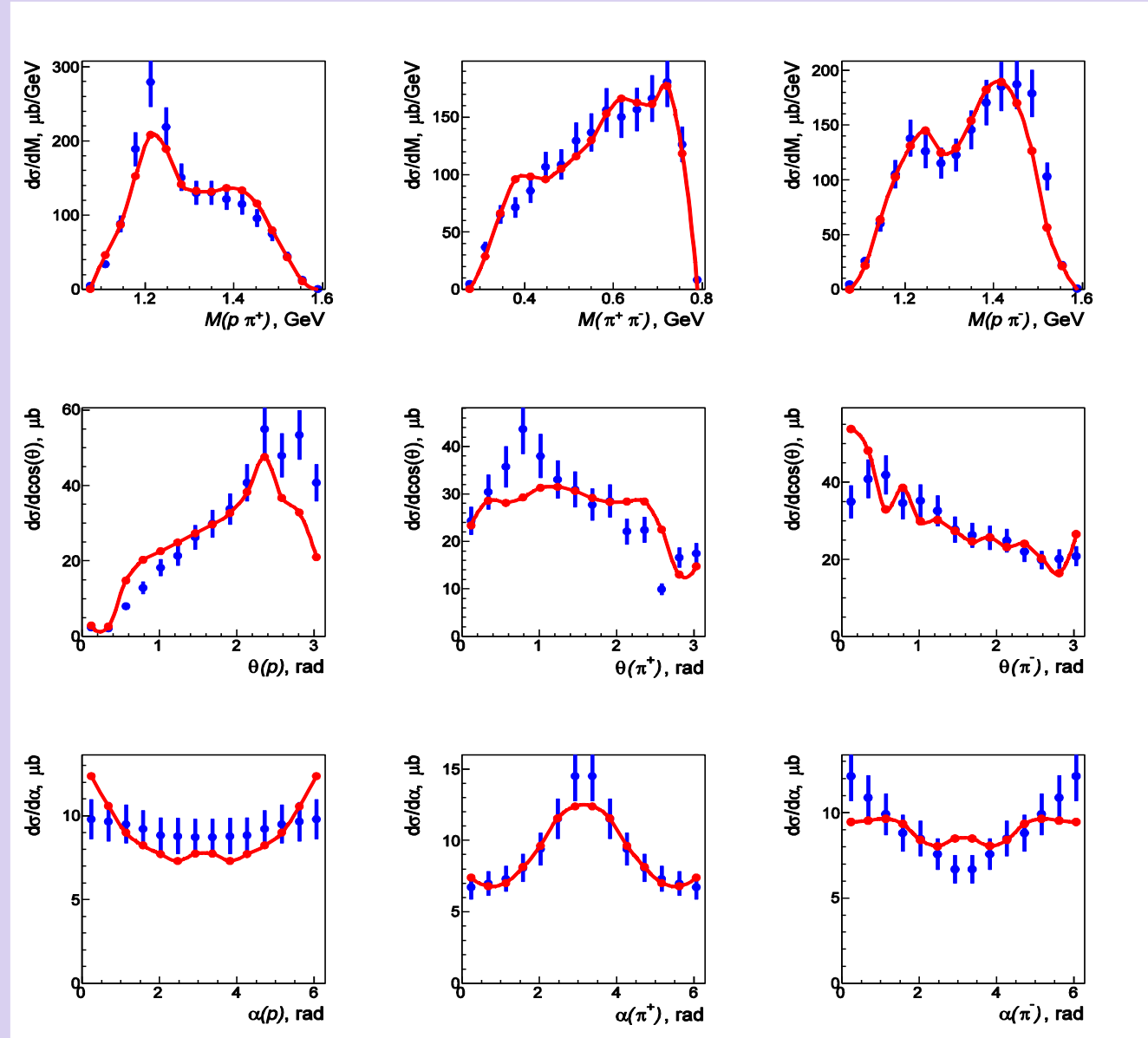
Dead zones: Model approach

Model can be used to account for dead area.

V.I.Mokeev et al., PRC 86, 035203 (2012).

First step:

The model was adjusted to the experimental cross section within CLAS acceptance



Dead zones: Model approach

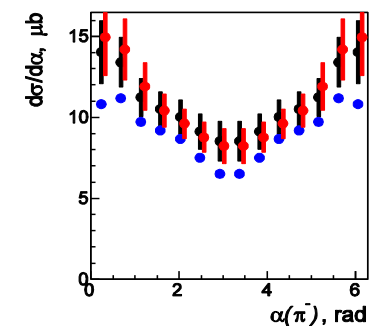
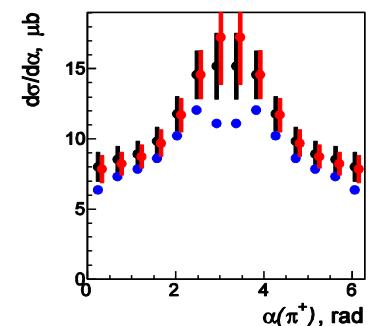
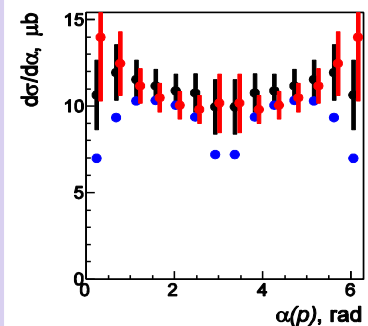
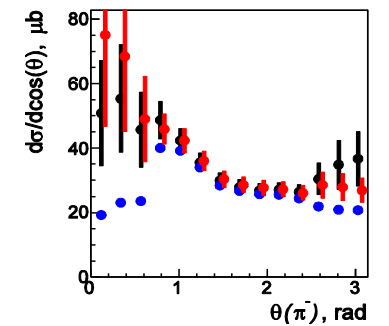
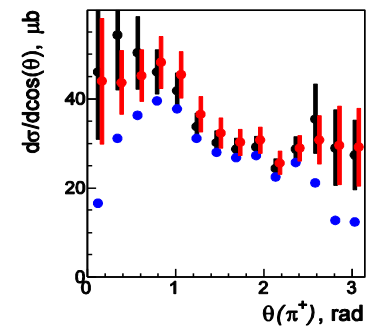
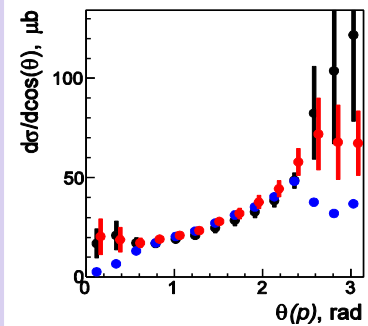
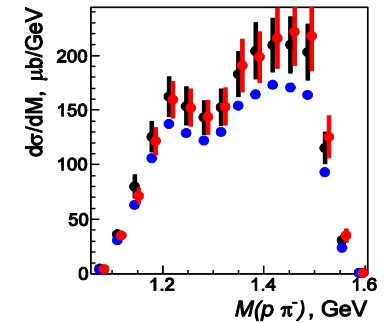
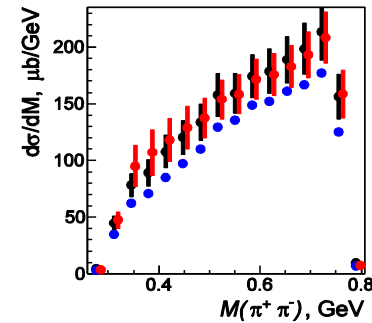
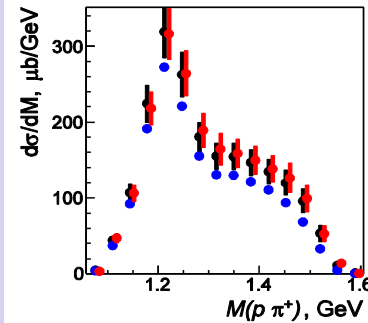
Second step:

extrapolation of the cross section into dead area with the model cross section

Cross sections within CLAS acceptance is in **blue**

Cross section accounted for dead area in simple approach is in **black**

Cross section accounted for dead area in model approach is in **red**

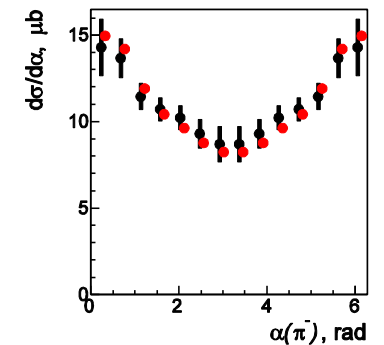
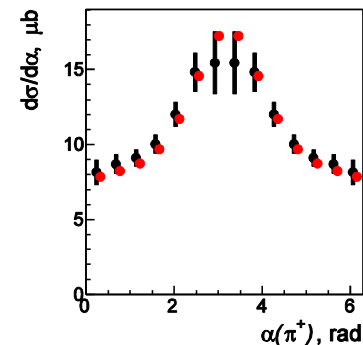
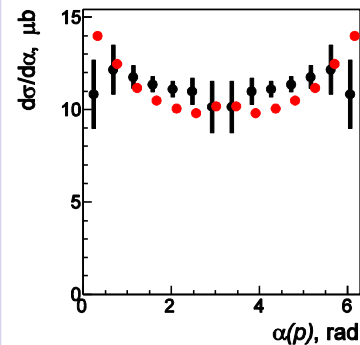
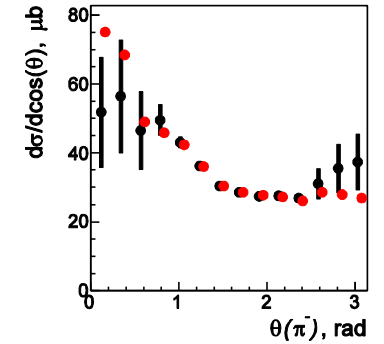
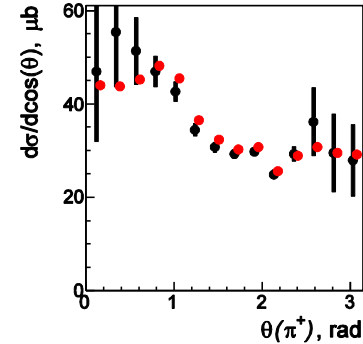
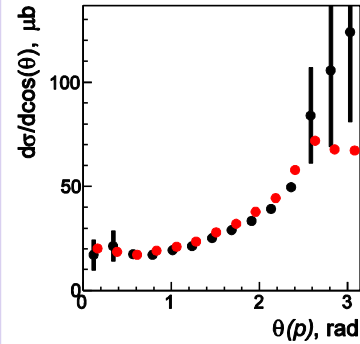
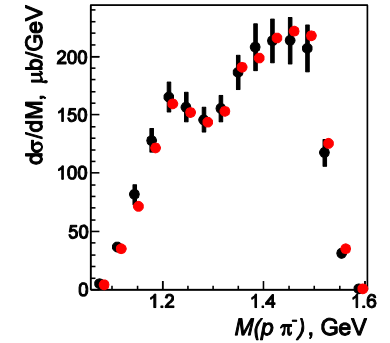
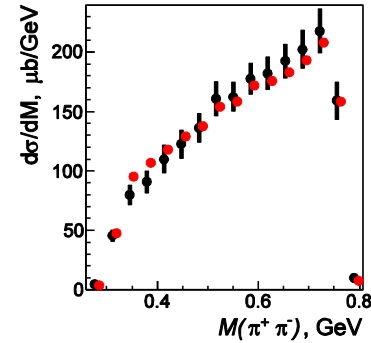
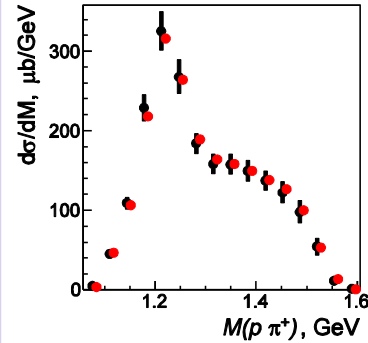


Dead zones: Model approach

Third step:

The model was adjusted to the cross sections obtained in the previous step in the full phase space of the reaction.

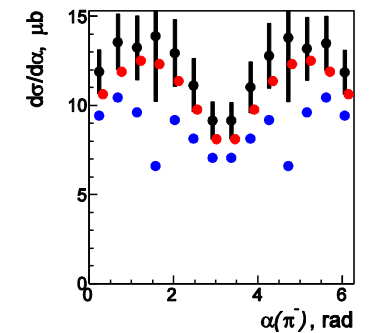
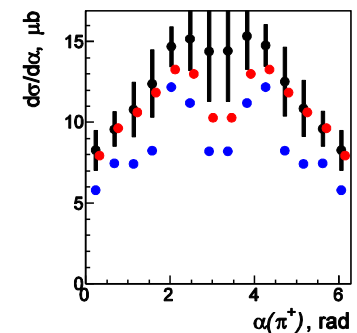
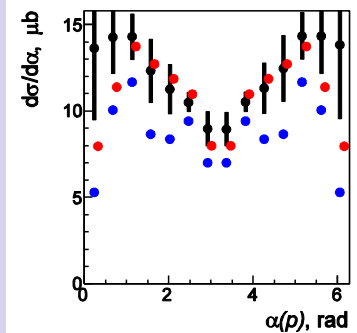
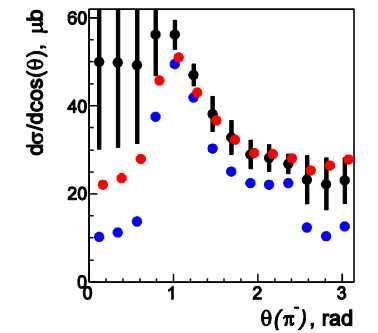
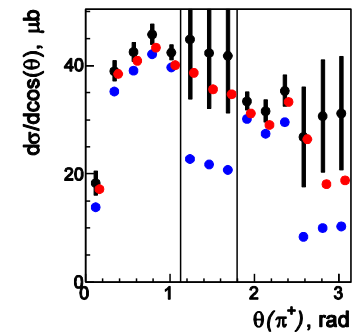
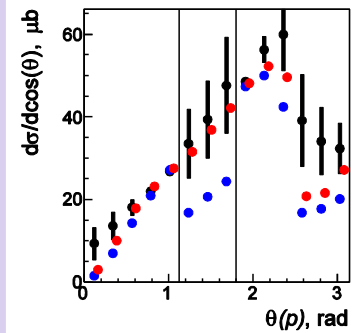
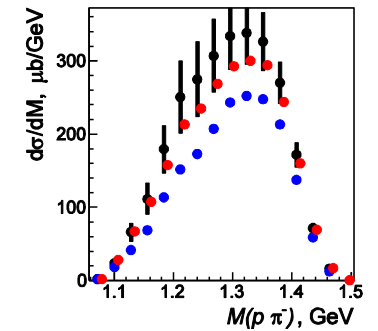
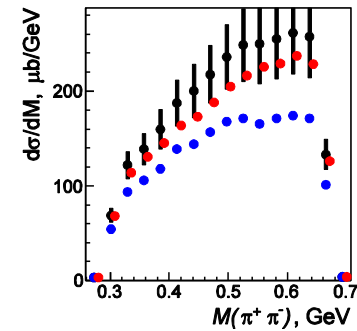
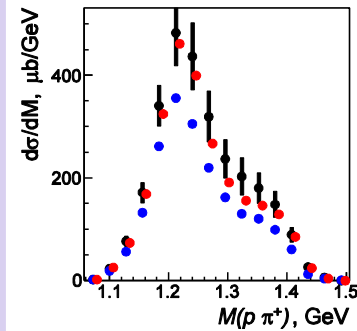
$1.6 \text{ GeV} < W < 2 \text{ GeV}$



Dead zones: Model approach: Extrapolation test

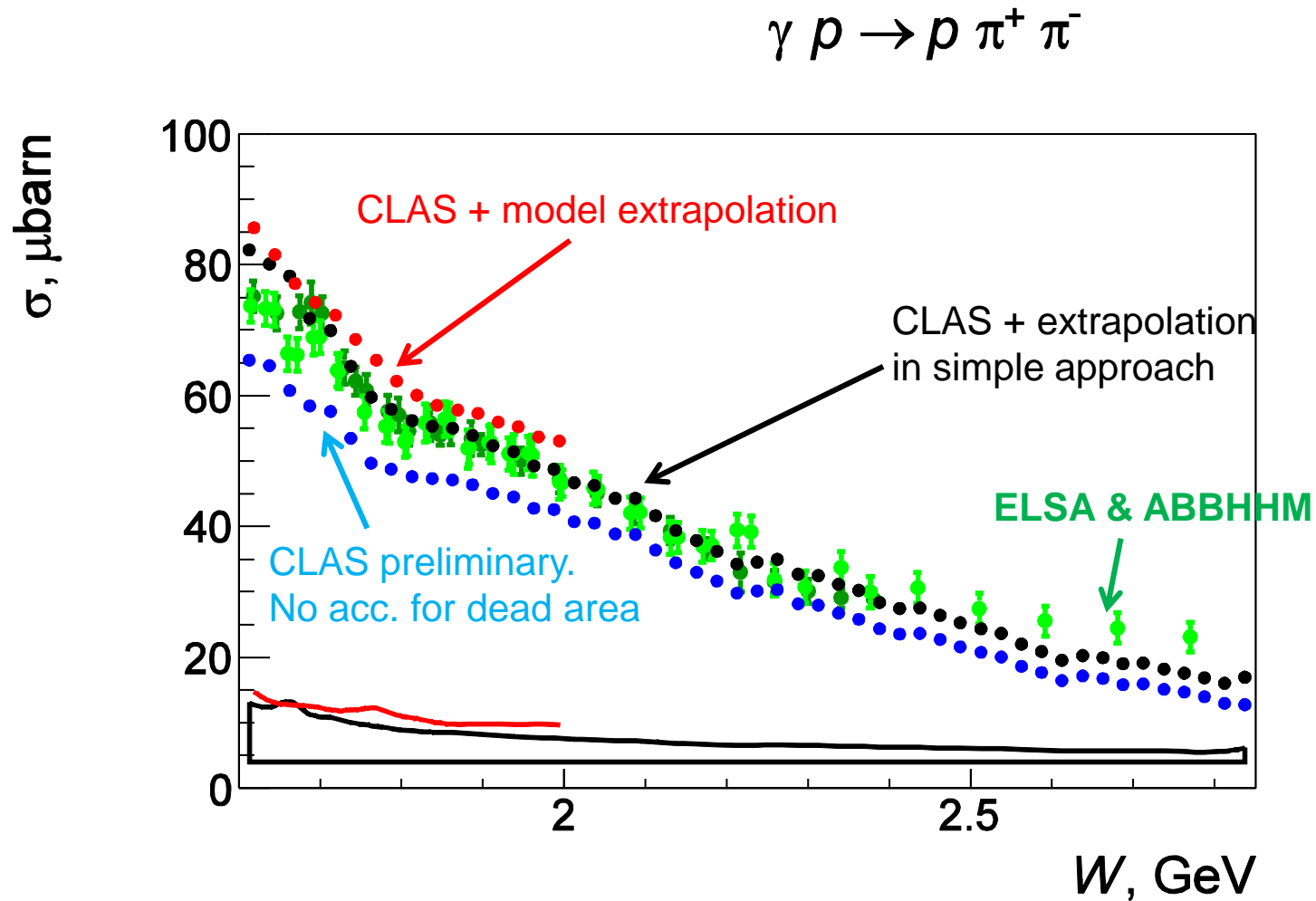
Extrapolation
Procedure test

Artificial dead area



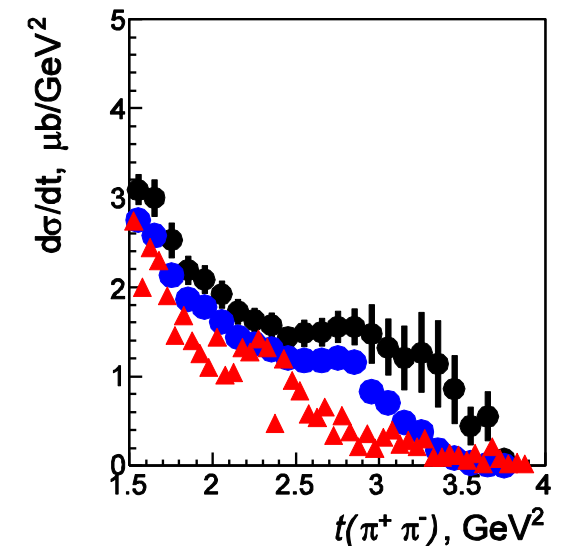
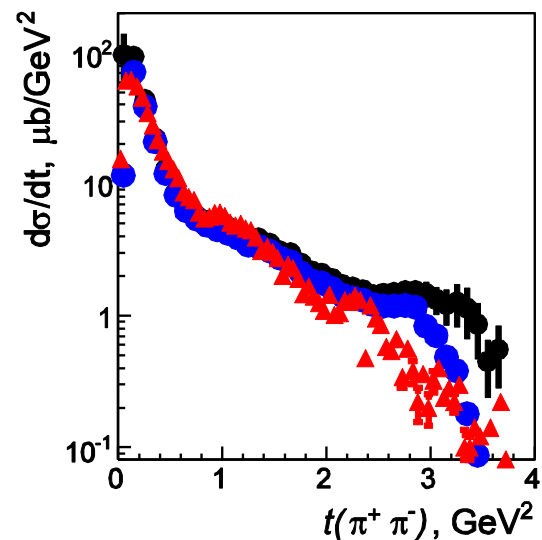
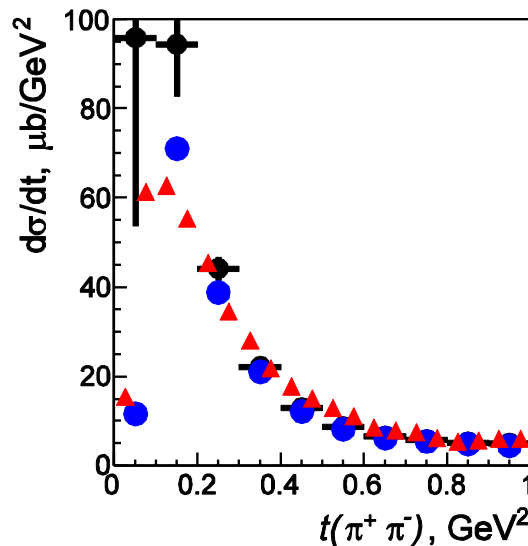
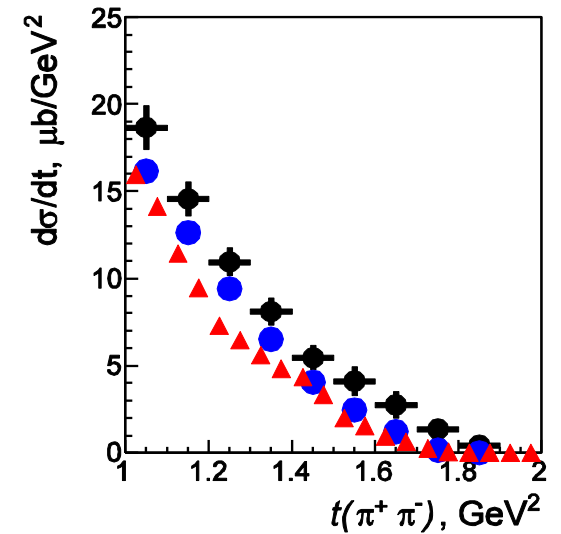
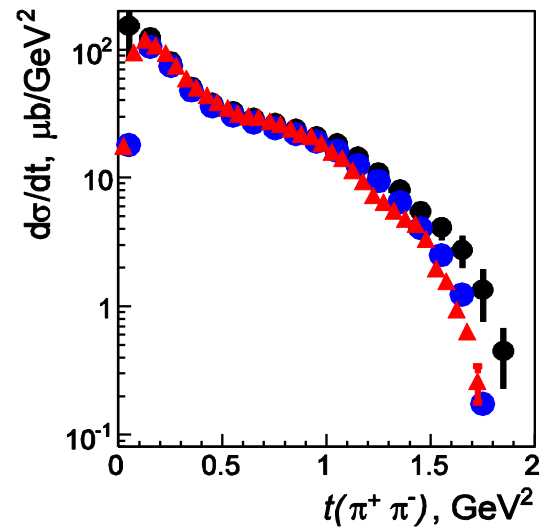
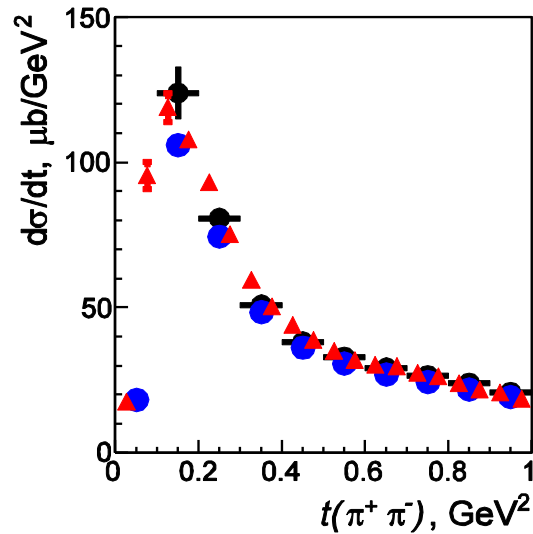
Cross section

Integrated two pion photoproduction cross section from CLAS G11



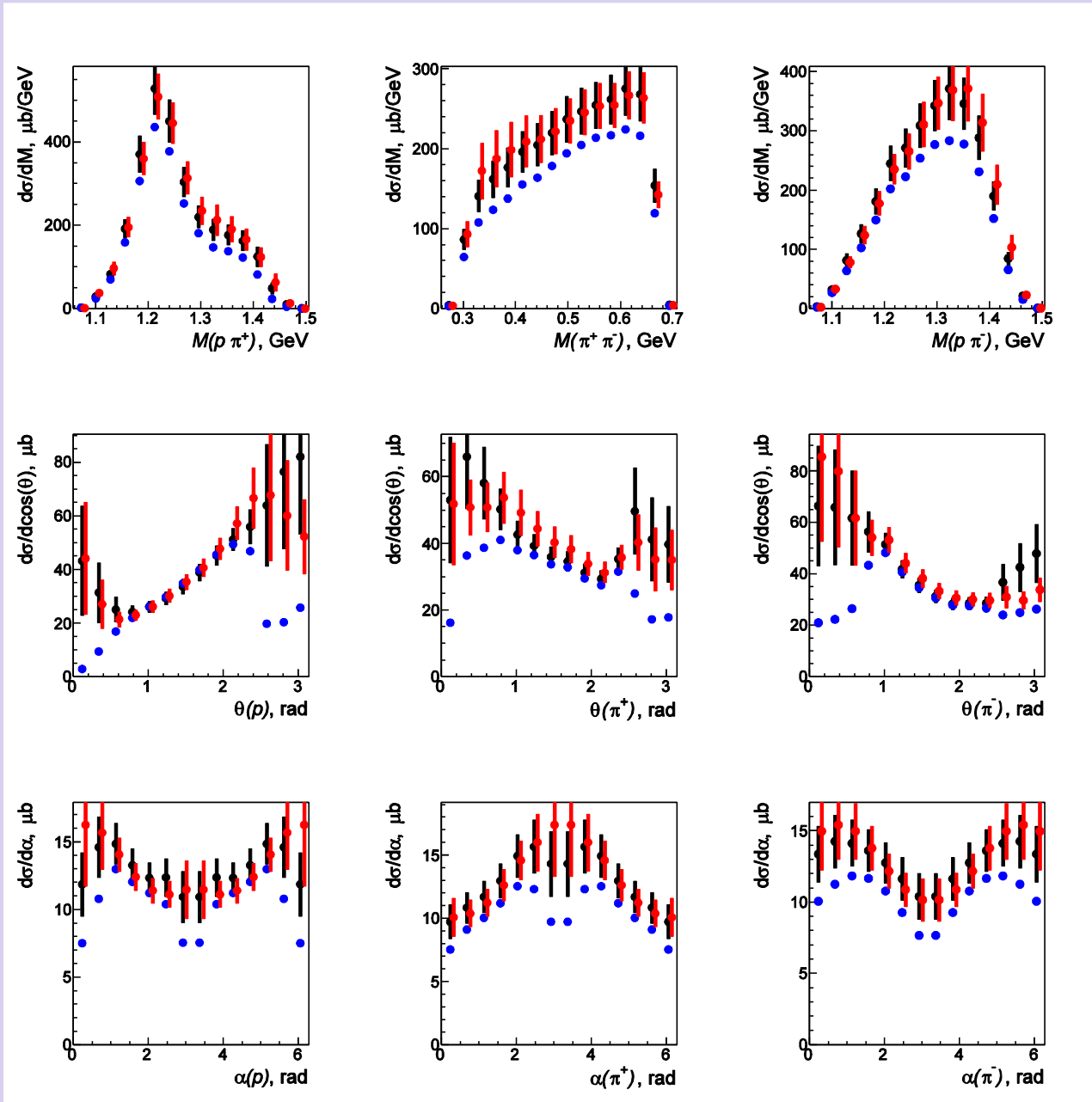
Cross section

Comparison of the differential over $t(\pi^+\pi^-)$ x-sections at $W=1.87$ and 2.37 GeV with SAPHIR data (*C. Wu et al. Eur.Phys.Jour. A23, 317 (2005)*)



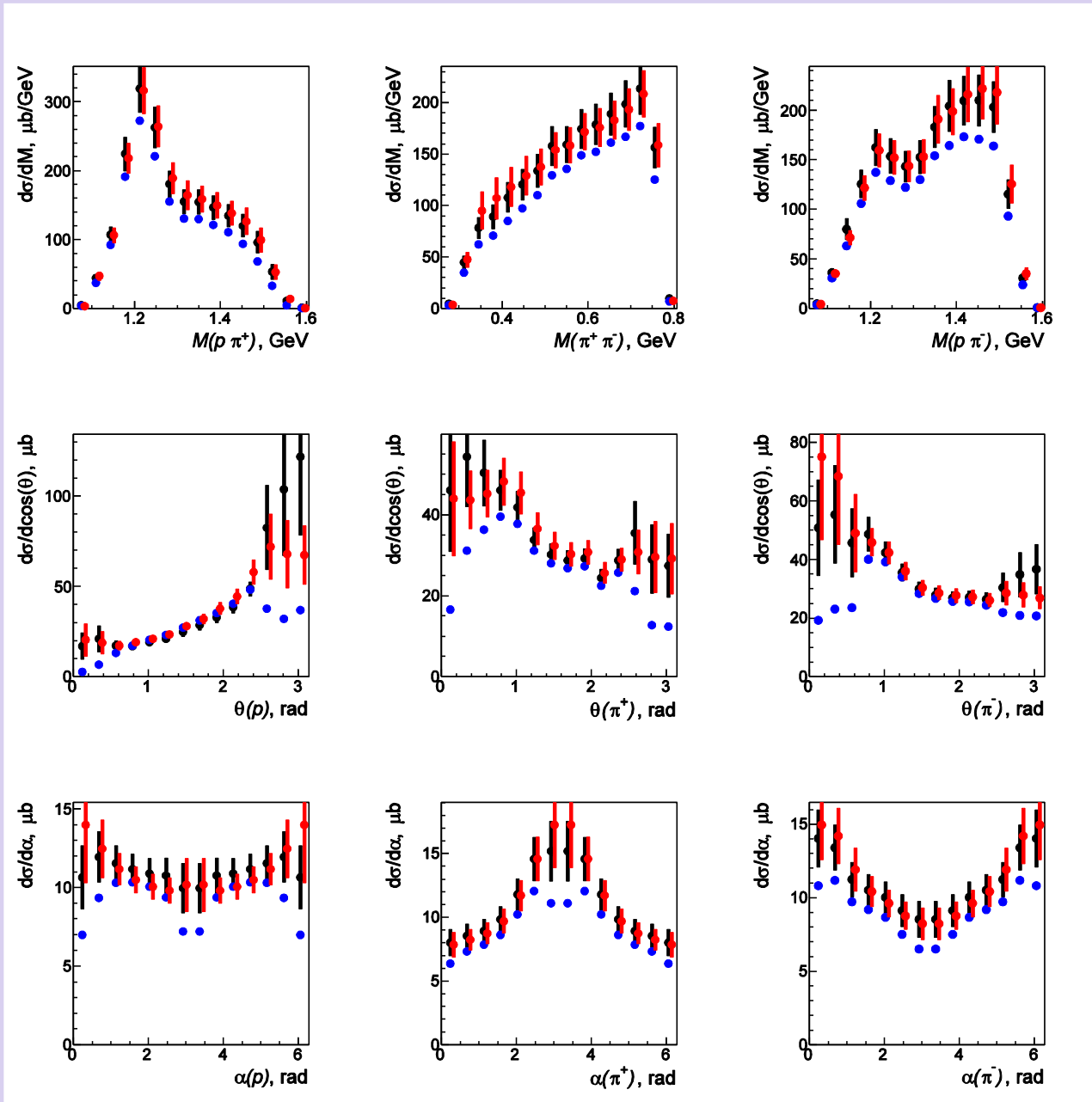
Cross section

Examples of the 1-fold differential x-sections at $W=1.61$ GeV



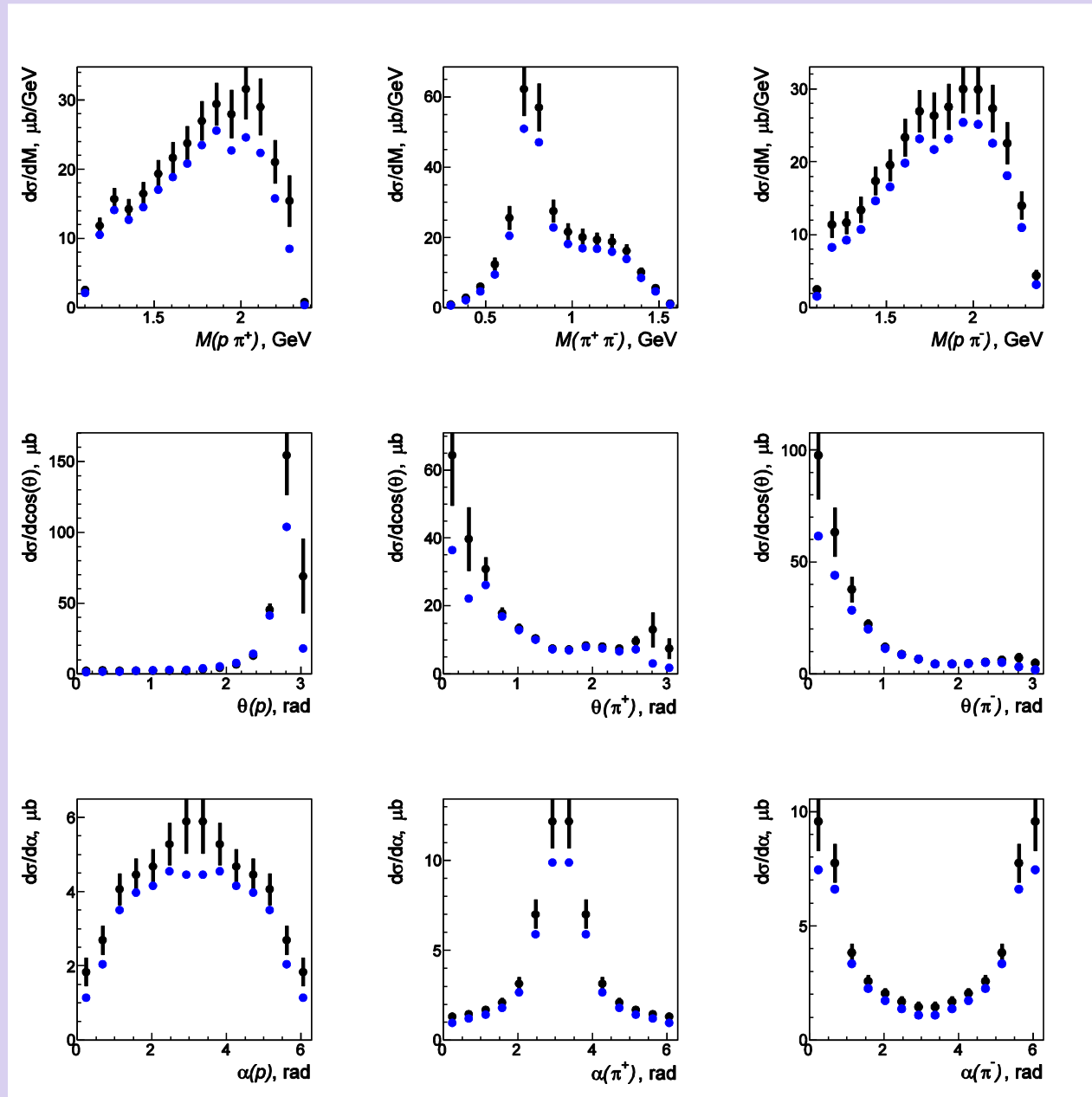
Cross section

Examples of the 1-fold differential x-sections at $W=1.71$ GeV



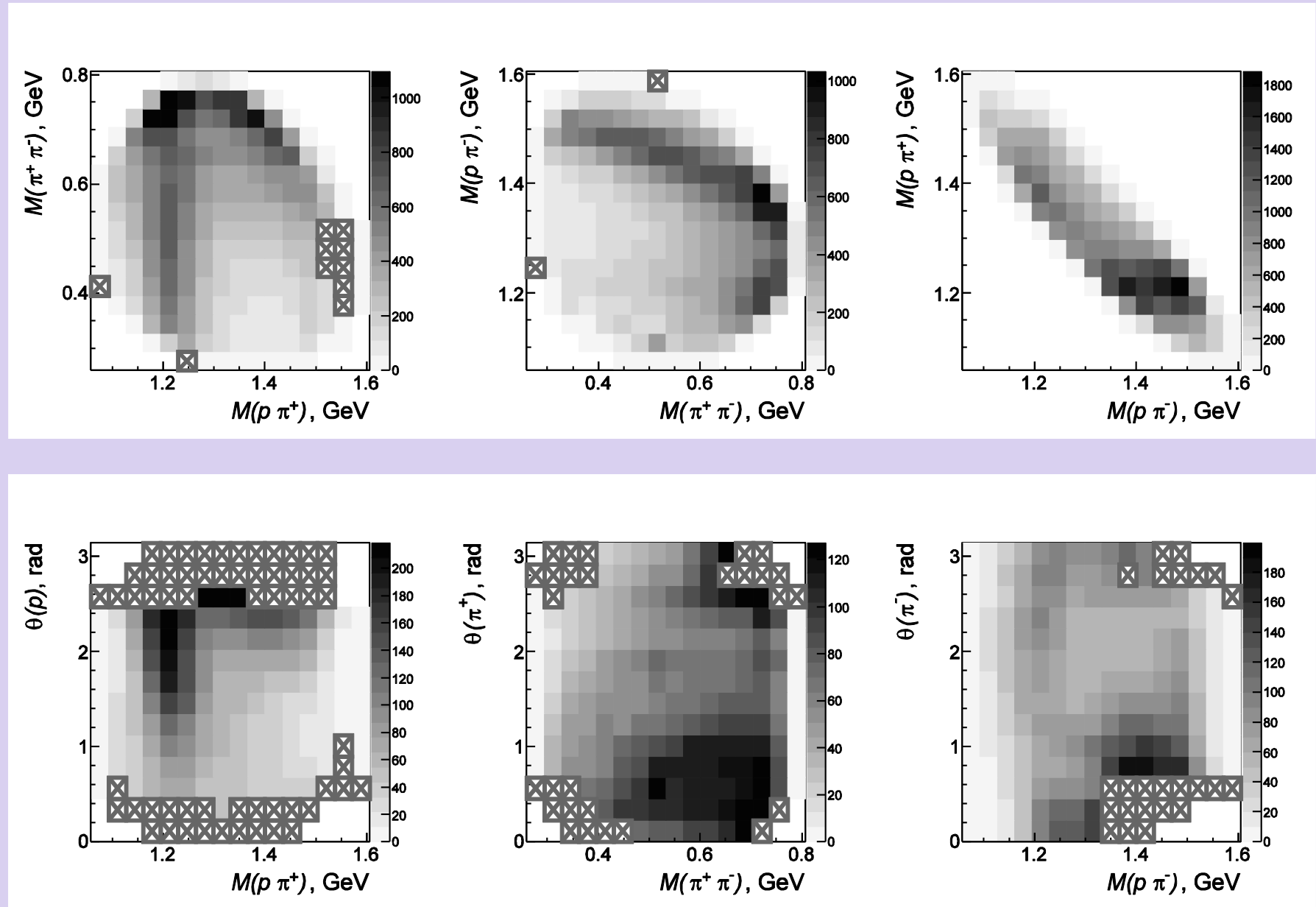
Cross section

Examples of the 1-fold differential x-sections at $W=2.51$ GeV



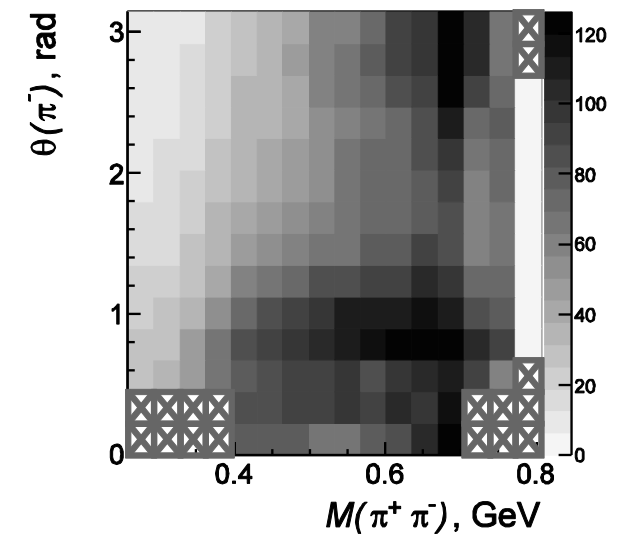
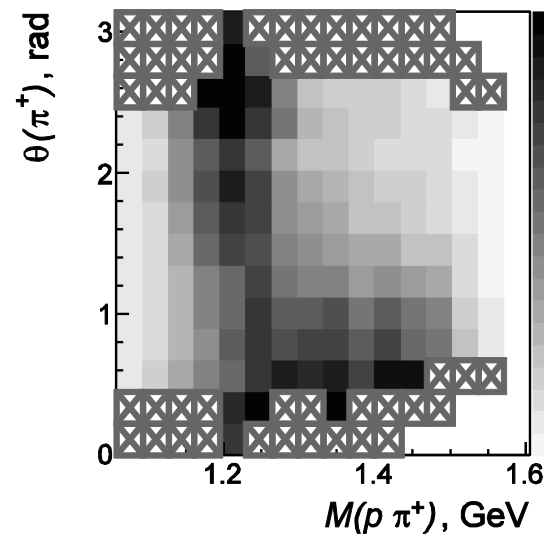
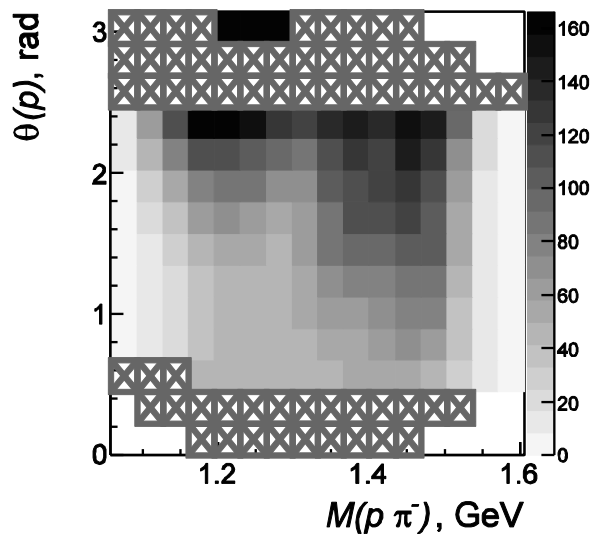
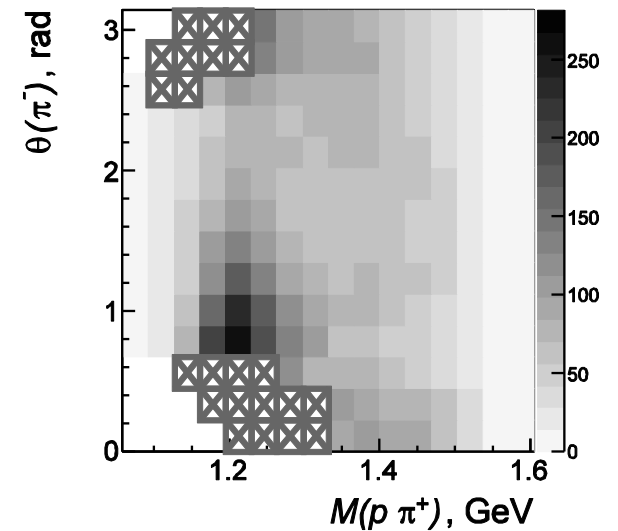
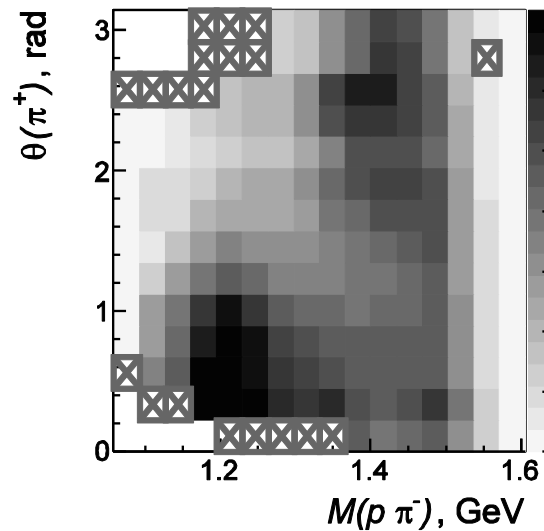
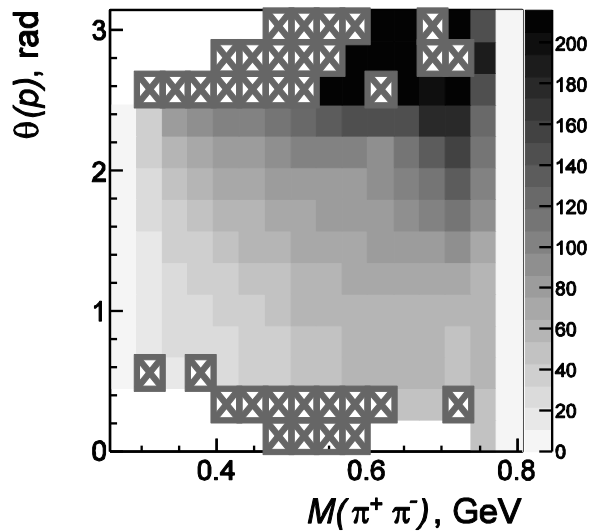
Cross section

Examples of the 2-fold differential x-sec. at $W=1.71$ GeV

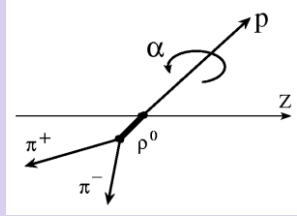


Cross section

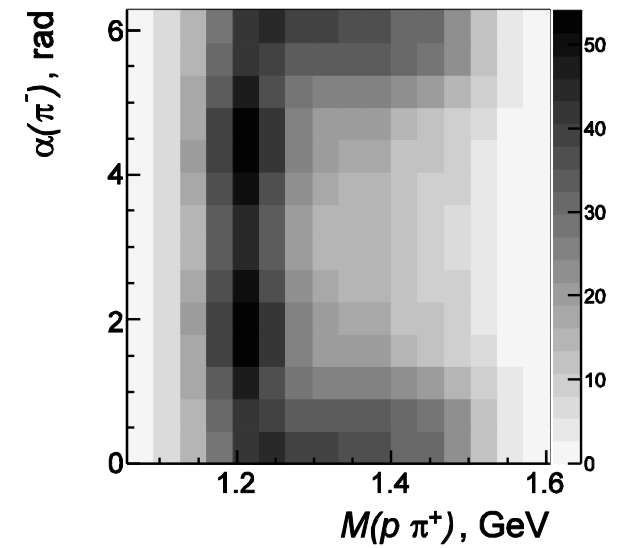
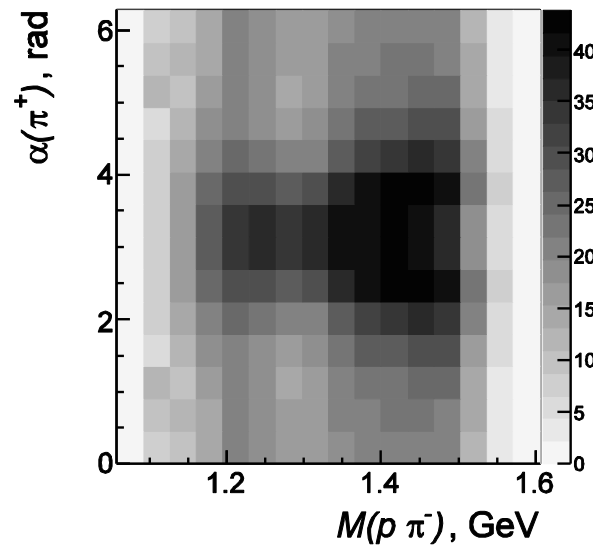
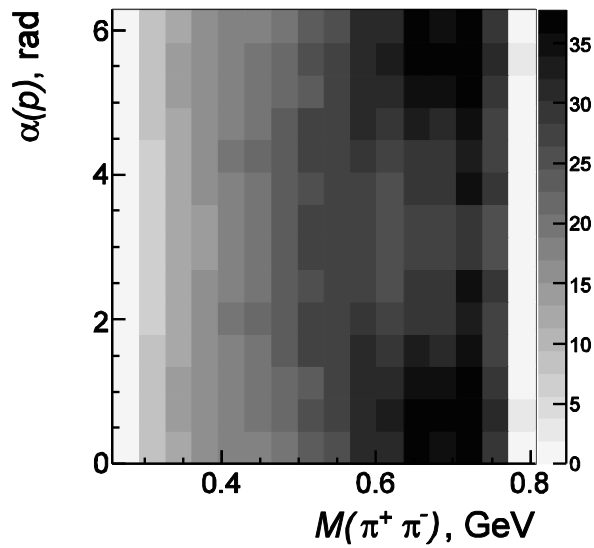
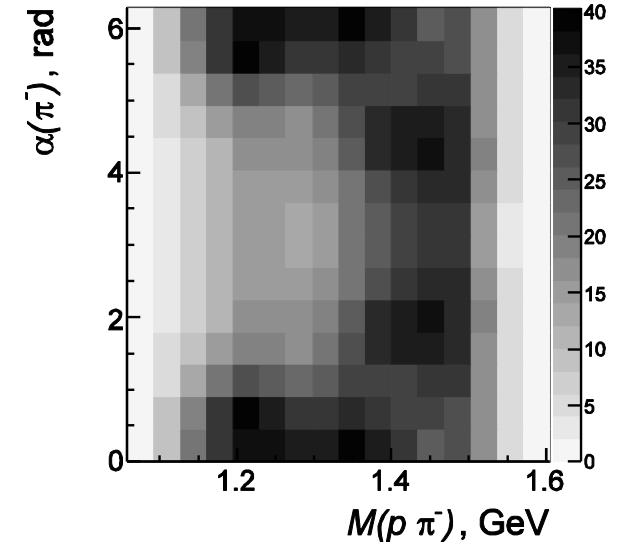
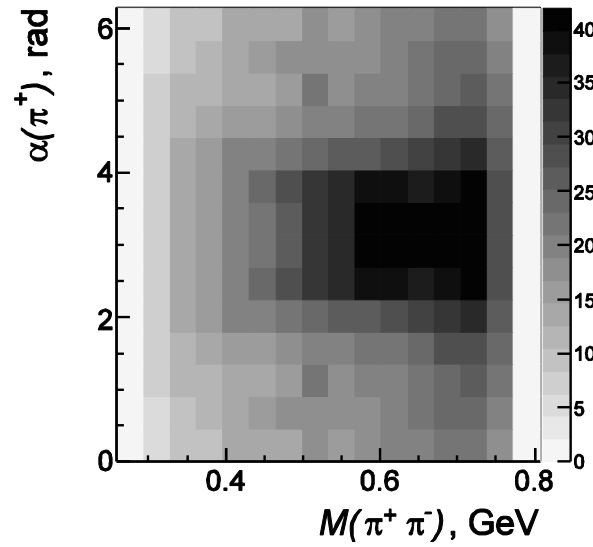
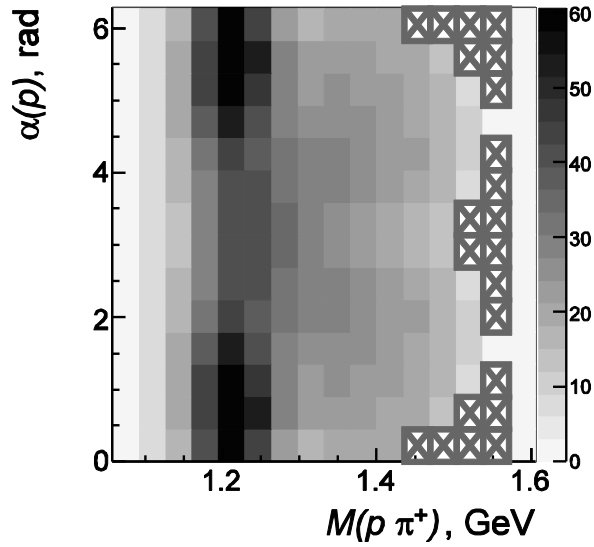
Examples of the 2-fold differential x-sec. at $W=1.71$ GeV



Cross section

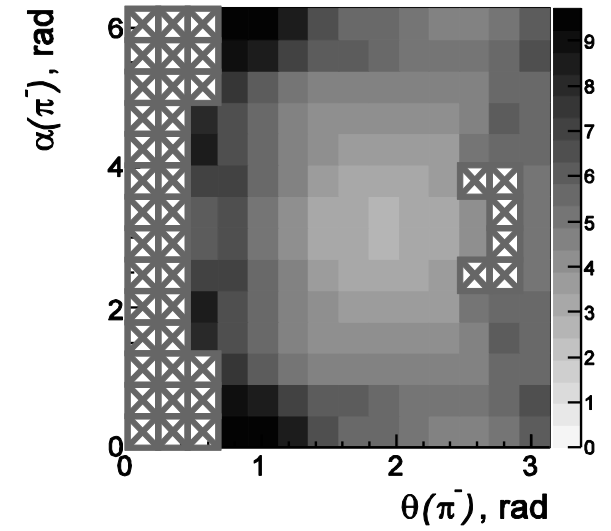
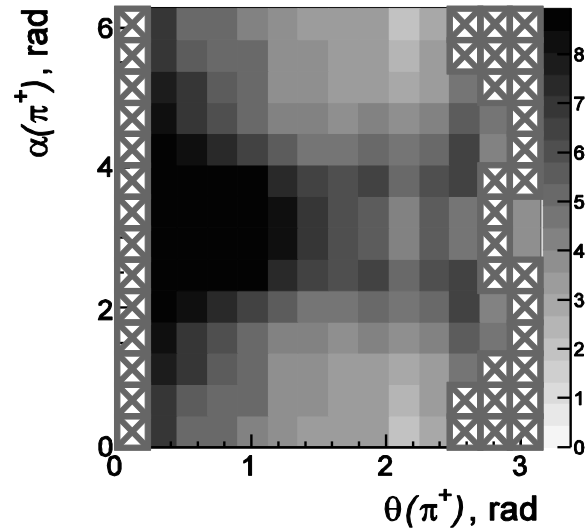
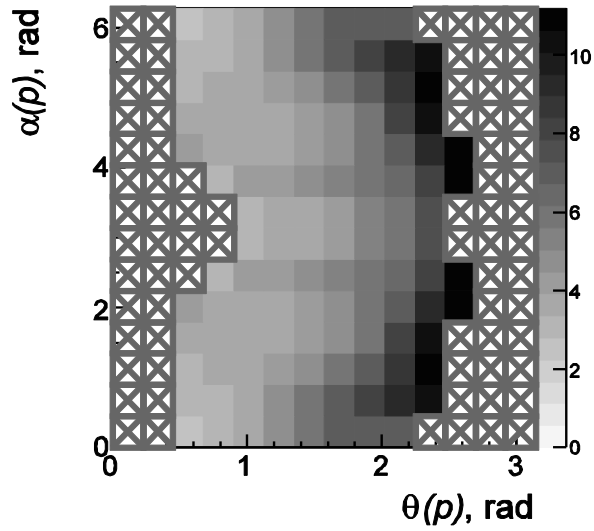


Examples of the 2-fold differential x-sec. at $W=1.71$ GeV



Cross section

Examples of the 2-fold differential x-sec. at $W=1.71$ GeV



First Interpretation of the structure at $W \sim 1.7$ GeV in $\pi^+\pi^-p$ electroproduction

The JM03 analysis of three 1-fold differential cross sections
(M.Ripani et al., PRL. 91, 022002 (2003)).

conventional states only, consistent with PDG 02

implementing $3/2^+(1720)$ candidate or conventional states only with different than in PDG 02 $N(1720)3/2^+ N\pi\pi$ decays.

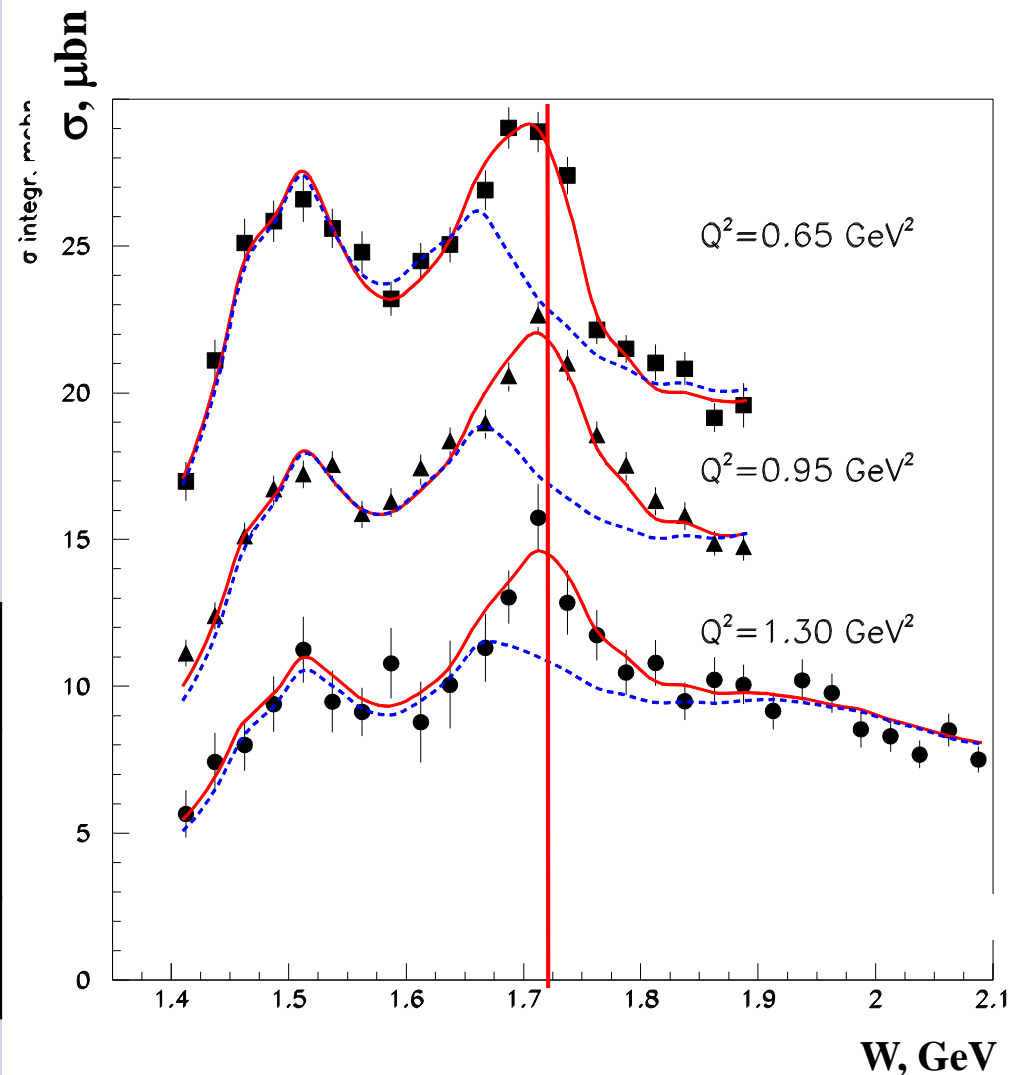
Two equally successful ways for the data description:

different than in PDG 02' $N(1720)3/2^+ N\pi\pi$ hadronic decay widths:

	Γ_{tot} , MeV	BF($\pi\Delta$) %	BF($\rho\rho$) %
$N(1720)3/2^+$ decays fit to the CLAS $N\pi\pi$ data	114 ± 19	63 ± 12 75 ± 12 (BnGa12)	19 ± 9
$N(1720)3/2^+$ PDG 02'	$150-300$	<20	$70-85$

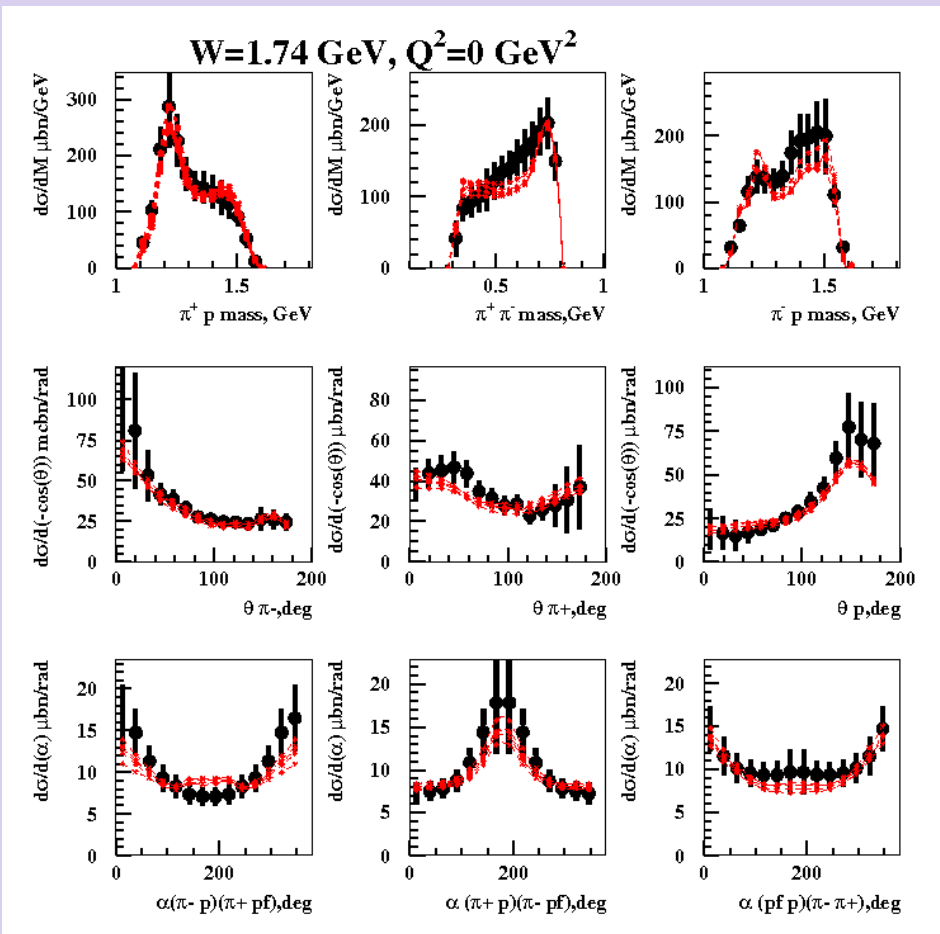
new $3/2^+(1720)$ state and consistent with PDG 02' $N\pi\pi$ hadronic decays of $N(1720)3/2^+$:

	Γ_{tot} , MeV	BF($\pi\Delta$) %	BF($\rho\rho$) %
$3/2^+(1720)$ candidate	88 ± 17	41 ± 13	17 ± 10
$N(1720)3/2^+$ conventional	161 ± 31	<20	$60-100$



Resonance photocouplings from the preliminary $\pi^+\pi^-p$ photoproduction cross sections

Fit of the CLAS data within the framework of the JM15:



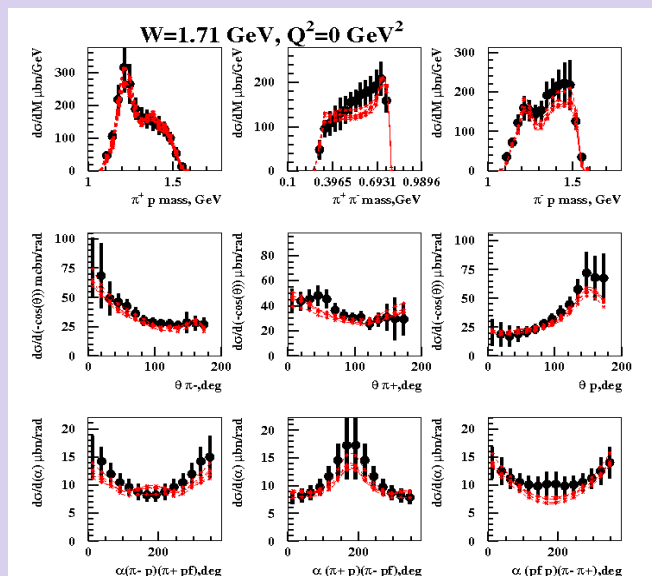
Resonance	$A_{1/2}$, GeV ^{-1/2} *1000, JM15/RPP12	$A_{3/2}$, GeV ^{-1/2} *1000 JM15/RPP12
N(1650)1/2 ⁻	63±6 53±16	
N(1680)5/2 ⁺	-29±3 -15±6	133±14 133±12
N(1700)3/2 ⁻	-5±4 -18±13	30±22 -2±24
N'(1720)3/2 ⁺	40±3 N/A	-43±8 N/A
N(1720)3/2 ⁺	89±16 97±3 (*)	-35±13 -39±3 (*)
Δ(1600)3/2 ⁺	-26±10 -23±20	-19±9 -9±21
Δ(1620)1/2 ⁻	33±4 27±11	
Δ(1700)3/2 ⁻	97±19 104±15	84±11 85±22
Δ(1905)5/2 ⁺	25±4 26±11	-57±10 -45±20
Δ(1950)7/2 ⁺	-68±16 -76±12	-123±20 -97±10

(*)M. Dugger et al., Phys. Rev. C76, 025211 (2007).

Consistent results on photocouplings of resonances with masses above 1.6 GeV from analyses of Np and $\pi^+\pi^-p$ channels demonstrate reliable extraction of these fundamental quantities.

Further evidence for the existence of the new state $N'(1720)3/2^+$ from combined $\pi^+\pi^-p$ Analyses in both photo- and electroproduction

Almost the same quality of the photoproduction data fit at $1.66 \text{ GeV} < W < 1.76 \text{ GeV}$ and $Q^2=0, 0.65, 0.95, 1.30 \text{ GeV}^2$ was achieved with and without $N'(1720)3/2^+$ new states



$N(1720)3/2^+$ hadronic decays from the CLAS data fit with conventional resonances only

N^* hadronic decays from the data fit that incorporates the new $N'(1720)3/2^+$ state

Resonance	BF($\pi\Delta$), %	BF(ρp), %
$N'(1720)3/2^+$ electroproduction photoproduction	47-64 46-62	3-10 4-13
$N(1720)3/2^+$ electroproduction photoproduction	39-55 38-53	23-49 31-46
$\Delta(1700)3/2^-$ electroproduction photoproduction	77-95 78-93	3-5 3-6

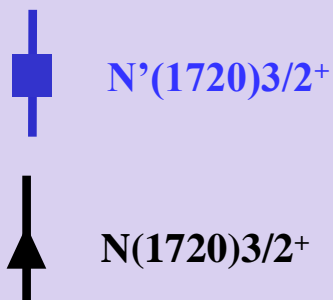
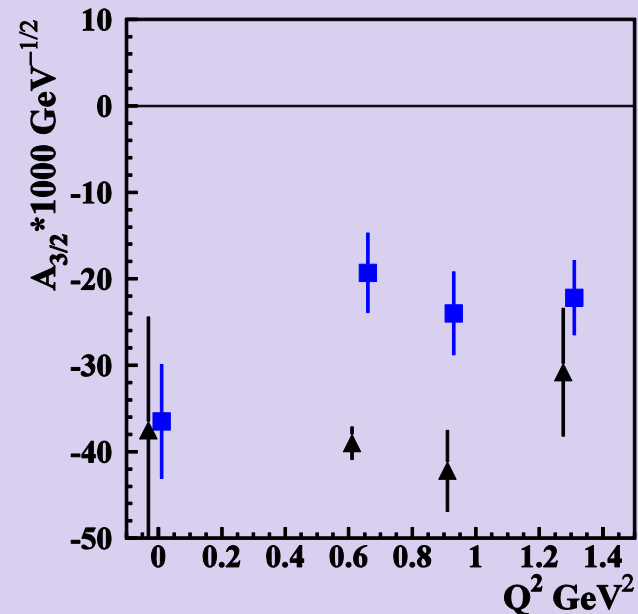
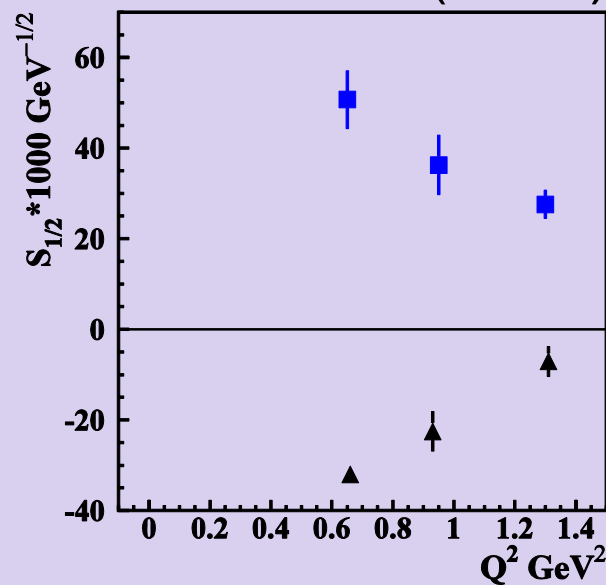
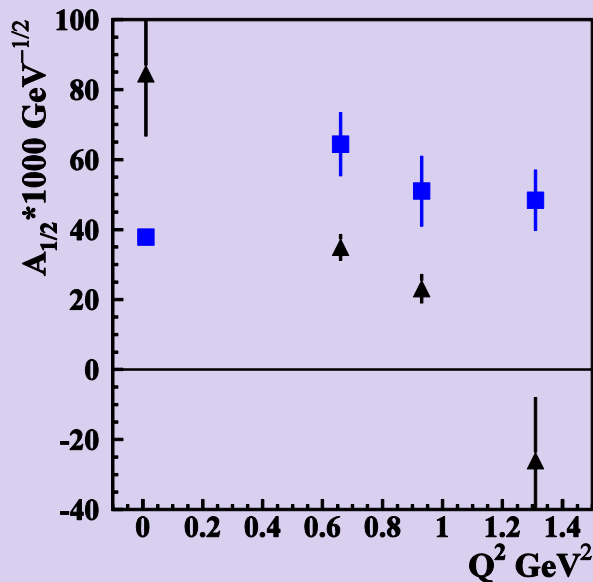
Successful description of $\pi^+\pi^-p$ photo- and electroproduction data achieved by implementing new $N'(1720)3/2^+$ state with Q^2 -independent hadronic decay widths of all resonances contributing at $W \sim 1.7 \text{ GeV}$ provides strong evidence for the existence of new $N'(1720)3/2^+$ state.

The contradictory BF values for $N(1720)3/2^+$ decays to the $\pi\Delta$ and ρp final states deduced from photo- and electroproduction data make it impossible to describe the data with conventional states only.

	BF($\pi\Delta$), %	BF(ρp), %
electroproduction	64-100	<5
photoproduction	14-60	19-69

The Parameters of $N'(1720)3/2^+$ New State from the CLAS Data Fit

The photo-/electrocouplings of $N'(1720)3/2^+$ and conventional $N(1720)3/2^+$ states:



Resonance	Mass, GeV	Total width, MeV
$N'(1720)3/2^+$	1.715-1.735	120 ± 6
$N(1720)3/2^+$	1.743-1.753	112 ± 8

$N'(1720)3/2^+$ is the only candidate state for which the results on Q^2 -evolution of transition electrocouplings have become available offering the insight to the structure of the new baryon state.

Conclusion and outlook

- ✓ Preliminary 1-fold and 2-fold differential $\pi^+\pi^-p$ photoproduction cross sections were extracted in W range 1.6-2.5 GeV
- ✓ Physics analysis of this data within the framework of reaction model developed in JLAB-MSU collaboration was performed in W range 1.6-2.0 GeV. Resonance photocouplings for the resonances with masses 1.6-2.0 GeV were extracted for the first time from the $\pi^+\pi^-$ -channel and they are in reasonable agreement with the values obtained in single pion photoproduction
- ✓ Successful description of $\pi^+\pi^-p$ photo- and electroproduction data achieved by implementing new $N'(1720)3/2^+$ state with Q^2 -independent hadronic decay widths of all resonances contributing at $W \sim 1.7$ GeV provides strong evidence for the existence of the new $N'(1720)3/2^+$ state
- ✓ Future combined analysis of photo- and electroproduction data for all relevant exclusive meson production channels is critical in order to confirm / rule out the signals of new baryon state observed in the photoproduction data